Analyst

Volume 1 | Number 1 | Jan 2013 | Pages 1–100

Analyst

www.rsc.org/analyst

ROYAL SOCIETY OF CHEMISTRY

www.rsc.org/analyst

Analyst

PAPER

A novel and versatile nanomachine for ultrasensitive and specific detection of microRNAs based on molecular beacon initiated strand displacement amplification coupled with catalytic hairpin assembly with DNAzyme formation [†]

Yurong Yan,[a] Bo Shen,[a] Hong Wang,[a] Xue Sun,[b] Wei Cheng,[c] Hua Zhao ,[b] Huangxian Ju[ad] and Shijia Ding*[a]

MicroRNAs are small regulatory molecules that can be used as potential biomarkers of clinical diagnosis, and efforts have been directed towards the development of a simple, rapid, and sequences-elective analysis for microRNAs. Here, we report a simple and versatile colorimetric strategy for ultrasensitive and specific determination of microRNAs based on molecular beacon initiated strand displacement amplification (SDA) and catalytic hairpin assembly (CHA) with DNAzyme formation. The presence of target microRNAs triggers strand displacement amplification to release nicking DNA triggers, which initiate CHA to produce large amount of CHA products. Meanwhile, the numerous CHA products can combine with hemin to form G-quadruplex/hemin DNAzyme, a well-known horseradish peroxidase (HRP) mimic, catalyzing a colorimetric reaction. Moreover, the purification of the SDA mixture has been developed for eliminating matrix interference to decrease nonspecific CHA products. Under the optimal conditions and using the promising amplification strategy, the established colorimetric nanomachine(biosensor) shows high sensitivity and selectivity in a dynamic response range from 5 fM to 5 nM with a detection limit as low as 1.7 fM (S/N=3). In addition, a versatile colorimetric biosensor has been developed for detection of different miRNAs by only changing the miRNA-recognition domain of molecular beacon. Thus, this colorimetric biosensor may become a potential alternative tool for biomedical research and clinical molecular diagnostics.

[a] Key Laboratory of Clinical Laboratory Diagnostics (Ministry of Education), College of Laboratory Medicine, Chongqing Medical University, Chongqing 400016, China.
[b] College of Pharmacy, Chongqing Medical University, Chongqing 400016, China.
[c] The Center for Clinical Molecular Medical detection, the First Affiliated Hospital of Chongqing Medical University, Chongqing 400016, China.
[d] State Key Laboratory of Analytical Chemistry for Life Science, Department of Chemistry, Nanjing University, Nanjing 210093, China.
* Corresponding author. Tel: +86-23-68485688; Fax: +86-23-68485786.
E-mail address: dingshijia@163.com (S.J.Ding) and dingshijia@cqmu.edu.cn
† Electronic Supplementary Information (ESI) available: Additional details of the experimental procedure and supplementary figures. See DOI: 10.1039/x0xx00000x

Introduction

Generally speaking, microRNAs (miRNAs) are a class of small (21-24 nt), endogenous, and non-coding RNA molecules.[1,2] The unnatural expression of miRNAs may lead to serious diseases, such as cancers,[3] nervous diseases,[4] and diabetes.[5] Particularly, the discovery of miRNAs in the cancers indicates that miRNAs may act as significant signaling molecules to regulate cancer development and progression and as potential biomarkers.[6,7]

Thus, quantitative analysis of miRNAs is crucial for better understanding their roles in cancer cells and further validating their function in biomedical research and clinical diagnosis.

MiRNAs have small size, vulnerable degradability, low abundance, and high sequence homology, thus crippling the traditional techniques for quantitative analysis of miRNAs.[8,9] Northern blot is widely utilized to visualize specific analysis of miRNAs expression, but it is semi-quantitative, low sensitivity, and requiring expensive equipment.[10] Microarray technology provides a strategy to analyze a little volume and multiple samples simultaneously. Nevertheless, its sensitivity and accuracy should also be ameliorated.[11] Real-time polymerase chain reaction (RT-PCR) has been established for sensitive analysis of miRNAs. However, it requires strict control of temperature cycling for successful detection, and generates false positive.[12] Therefore, developing highly efficient signal amplification strategy for simple, specific, and sensitive determination of miRNAs is in urgent need.

For highly sensitive detection of miRNAs, the emerging research field of isothermal nucleic acid amplification, such as strand displacement amplification (SDA),[13-15] rolling circle

amplification (RCA),[16-18] loop-mediated amplification (LAMP),[19,20] exonuclease III-assisted target recycling amplification (ERA),[21-23] and signal mediated amplification of RNA technology (SMART),[24] may be much more simple than the polymerase chain reaction (PCR) for the amplification of nucleic acid analysis. However, the efficient detection of amplicons becomes analytically difficult and in many cases still relies on the detection of final products, which usually are identified by electrophoresis with dye staining (using ethidium bromide or SYBR Green). In addition, these methods can be deprived of specificity because any accumulation of parasitic or nonspecific amplicons yields a false-positive.[25] In contrast, nonenzymatic nucleic acid circuits, such as CHA,[26,27] hybridization chain reactions (HCR),[28-30] RNA cleaving deoxyribozymes,[31] and template-directed chemical reaction,[32] have provided efficient methods for amplicons detection of isothermal nucleic acid amplification. Of these circuits, CHA has been proven to be useful in amplifying and transducing signals at the terminus of nucleic acid amplification reactions.[33,34] What is more, CHA has been engineered to yield hundreds-fold catalytic amplification with negligible background and can transduce analyte signal binding to various detection modalities, such as fluorescent, colorimetric, and optic signals.[33,34] Therefore, CHA can be utilized as the specific end-point transducer for development of enzyme-free based isothermal amplification strategies.

Inspired by these strategies, our motivation herein is to design a versatile naomachine for detection of low abundance miRNAs by coupling SDA and CHA with DNAzyme formation. Although the amplification signal is derived from the end-products (DNAzyme) of the DNA nanomachine, the process is continuously amplified through the SDA, CHA, and hairpin recycling assembly during the operation. More importantly, the presence of target miRNAs can trigger the operation of the DNA machine. Meanwhile, the amplification nanomachine can transform the input of target miRNAs into numerous outputs of DNAzyme, thus produce green ABTS$^{•-}$ for sensitive colorimetric and visual detection of miRNAs. This machine provides a simple, versatile, and sensitive platform for different miRNAs determination and may become a potential tool for clinical molecular diagnostics.

Experimental

Reagents

Klenow fragment (3′-5′ exo) and Nb.BbvCI were purchased from New England Biolabs (Beijing, China). Hemin and 2, 2′-azino-bis (3-ethylbenzothiazoline-6-sulfonic acid) (ABTS^{2-}) were purchased from Sigma-Aldrich (St. Louis, MO, USA). 20 bp DNA Ladder Marker, ethanol precipitation kit, RNase inhibitor, and miRNAs were obtained from TaKaRa Biotech. Inc. (Dalian, China). Hydrogen peroxide (H$_2$O$_2$), bovine serum albumin (BSA), diethylpyrocarbonate (DEPC), deoxynucleotide solution mixture (dNTPs), and DNA oligonucleotides were obtained from Sangon Biotechnology Co. Ltd. (Shanghai, China). The sequences of nucleic acids employed in this study are shown in ESI, Table S1[†]. All oligonucleotides were dissolved in tris-ethylenediaminetetraaceticacid (TE) buffer (pH 8.0, 10 mM Tris-HCl, 1 mM EDTA) and stored at -20 °C, which were diluted in appropriate buffer prior to use.

The stock solution of 1.0 μg/μL total RNA extracted from breast adenocarcinoma (MCF-7) cells was purchased from Ambion (California, USA). All solutions and deionized water used were treated with diethyprocarbonated (DEPC) and autoclaved to protect from RNase degradation. All other reagents were of analytical grade. All aqueous solutions were prepared using Millipore-Q water (≥18MΩ, Milli-Q, Millipore). Hemin stock solution (4 mM) was prepared in dimethyl sulfoxide (DMSO) and stored in the dark at -20 °C. The stock solution of hemin was diluted to the required concentration with 0.1M KCl in pH 7.4, 0.01 M PBS buffer.

Apparatus

A UV-visible spectrophotometer (UV-2550, Shimadzu, Kyoto, Japan) was used to monitor the colorimetric signal. The concentrations of DNA suspensions were measured using a NanoDrop 1000 spectrophotometer (Thermo Scientific, Wilmington, DE, USA). The gel electrophoresis was performed on the DYY-6C electrophoresis analyzer (Liuyi Instrument Company, China) and imaged on Bio-rad ChemDoc XRS (Bio-Rad, USA).

Preparation of probes

Molecular beacon (MB), hairpin H1, and hairpin H2 were designed by the rule and principle of the enzyme-free strand-displacement systems and referring to the published work.[13,25] In order to avoid the polymerization of the MB, MB was modified with five adenines and C6 Spacer in the 3'end of MB (ESI, Table S1 and Fig. S1[†]). All hairpin probes were heated to 95 °C for 5 min, followed by gradually cooling down to room temperature. The obtained DNA solutions were then stored at 4 °C for further use.

Assay protocol for target miRNAs

The strand displacement amplification reaction was initiated by addition of 5 μL target miRNAs with various concentrations, 10 μL of 100 nM different MB probes, 1 μL of 0.1 U/μL Klenow fragment, 1 μL of 0.2 U/μL Nb.BbvCI, 1.2 μL of 250 μM dNTP, 1.5 μL of 1.2 U/μL RNase inhibitor, 5 μL NEBuffer 2 (10 mM pH 7.9 Tris-HCl, 50 mM NaCl, 10 mM MgCl$_2$, 1 mM DTT), 5 μL CutSmart™ Buffer (20 mM pH 7.9 Tris-acetate, 500 mM potassium acetate, 10 mM magnesium acetate, 100 μg/mL BSA) and 20.3 μL DEPC-treated water. Final volume was 50 μL. Then the SDA reaction was conducted at 37 ºC for 80 min. Next, the resulted products were purified by ethanol precipitation (ESI). Finally, the precipitation pellet was dissolved in 75 μL TNAK buffer (20 mM pH 7.5 Tris-HCl, 125 mM NaCl, 20 mM KCl).

CHA amplification reaction was triggered by addition of 75 μL upstream SDA mixture, 75 μL of 75 nM H1 and 50 μL of 50 nM H2 in the TNAK buffer and incubated for 60 min at 37 ºC. Finally, 3 μL of 3 μM freshly prepared hemin solution was added into the products, and the mixture was incubated at room temperature (RT) for 30 min to form a lot of DNAzymes through the interaction between hemin and G-quadruplex. 200 μL aliquot of 4 mM $ABTS^{2-}$ and 1 μL aliquot of 30% H_2O_2 were added to the reaction mixture and incubated at RT for 5 min. The absorbance of the mixture was measured at 418 nm, and the absorbance spectra was measured using a UV-visible spectrophotometer in the wavelength range from 500 to 400 nm against a blank.

Results and discussion

Design of the machine for miRNAs detection

The principle of DNA nanomachine for ultrasensitive determination for miRNAs by integrating SDA and CHA is illustrated in Scheme 1 and ESI, Fig. S1[†]. The versatile MB template consists of three domains: a miRNA-recognition domain (depending on target) (a), a nicking domain for Nb.BbvCI recognition (b), and an amplification domain for producing the nicking triggers (c). The amplification domain is designed for SDA, which produces the nicking triggers to initiate the following CHA. In the presence of target miRNAs, the specific hybridization of miRNAs with domain (a) opens the circular part of MB, and the bound miRNAs is extended along domain (b) and domain (c) to form a complete duplex by Klenow fragment. Subsequently, the Nb.BbvCI specifically recognizes the duplex nicking site to cleave the extended DNA strand at domain (b), releasing the nicking triggers. Upon the circulation of the extension and cleavage processes at domain (c), a number of nicking triggers are released as to initiate the downstream CHA. Amounts of nicking DNA triggers catalyze the automatic assembly of H1 and H2 to produce numerous CHA products. Meanwhile, the formation of the CHA products can cause the release of the DNA triggers, thereby promoting the hairpin recycling assembly. Because of the G-quadruplex at the 5' end of H1, DNAzyme can be formed upon addition of hemin. The DNAzyme formed by the SDA-CHA products can act as peroxidase mimics to catalyze the $ABTS^{2-}$-H_2O_2 system, thus resulting in the amplification of the colorimetric detectable signals. More importantly, a versatile colorimetric biosensor has been developed for detection of different miRNAs by only changing the miRNA-recognition domain of MB.
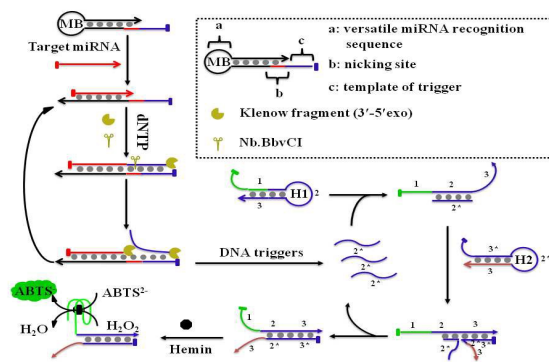
Scheme 1 Schematic representation of the nanomachine for target miRNAs detection by the versatile MB template including a versatile miRNA-recognition domain (a), a nicking domain for Nb.BbvCI recognition (b) and an amplification domain for producing the nicking triggers (c).

Characterization of the nanomachine

To verify our design, one precondition for the nanomachine was whether the purified SDA products could trigger the CHA for the formation of DNAzyme. UV-vis absorbance spectra, in the substrate solution containing hemin and $ABTS^{2-}$-H_2O_2, were monitored using 5 nM miRNAs before and after incubation with H1 or H2 (Fig. 1A). As a control experiment, the mixture containing hemin and $ABTS^{2-}$-H_2O_2 was investigated (curve 'a'). A weak absorbance was observed at 418 nm, indicating that hemin alone could generate a low catalytic efficiency toward $ABTS^{2-}$-H_2O_2 without the formation of DNAzyme. Significantly, when only H1 in the mixture containing hemin and $ABTS^{2-}$-H_2O_2, the absorbance (curve 'b') exhibited almost no change relative to curve 'a', suggesting that the added hemin could not trigger the opening of H1 to form the DNAzyme. In addition, when H1 and H2 coexisted in the mixture containing hemin and $ABTS^{2-}$-H_2O_2, the absorbance (curve 'c') showed almost no change relative to curve 'a', demonstrating that hairpins H1 and H2 coexistence could not breathe to form the DNAzyme. In contrast, after the purified SDA products were incubated with H1, hemin, and $ABTS^{2-}$-H_2O_2, the absorbance (curve 'd') increased relative to curve 'a'. The reason might be that the catalytic sequence carried within the purified SDA products could stimulate the opening of H1 to form the DNAzyme. Meanwhile, the phenomenon could be further verified from curve 'e' in the coexistence of H1 and H2. Compared with the absorbance shown by curve 'c', the strong absorbance achieved was contributed to H2, indicating use of H2 can induce the hairpin recycling assembly in the presence of the purified SDA products. The insets of Fig. 1A showed the corresponding photographs, which were in accordance with results obtained by UV-vis absorption spectra.

Another question appeared as to whether the purified SDA products could be generated in the presence of target miRNAs. To clarify this issue, a native polyacrylamide gel electrophoresis (PAGE) experiment (ESI) was carried out. As shown in Fig. 1B, the distinct band of 29 nt, representing the purified SDA products, was observed with the addition of target miRNAs (Fig. 1B, lane 3). However, the purified SDA products could not be observed in the control group without the addition of target miRNAs or Nb.BbvCI (Fig. 1B, lane 1 or lane 2). These results indicated that in the presence of target miRNAs, the versatile nanomachine could generate the purified SDA products to trigger CHA for the formation of DNAzyme.

To achieve the effective combination of SDA and CHA and obtain high-quality CHA DNA circuits, we investigated whether the matrix of the SDA reaction mixture affected the CHA reaction. As shown in Fig. 1C and Fig. 1D, upon the same experiment condition, the signal to noise of 5 nM and 50 fM miRNAs for the purified SDA products was 3.5 and 1.7, respectively (Fig. 1C). However, the signal to noise of 5 nM and 50 fM miRNAs for not purified SDA product was only 2.1 and 1.0, respectively (Fig. 1D). The reason might be attributed to the background leakage caused by a number of factors, including the purity of the DNA samples and the misfolding of

nucleic acids into alternative conformers.[35,36] Meanwhile, the absence of Mg^{2+} in the matrix of SDA reaction should also disfavor non-specific reactions, leading to more than 200-fold lower background reactivity of our circuit.[33] Thus, to enhance the efficiency of CHA, the SDA reaction mixture should be purified for decreasing background signal.
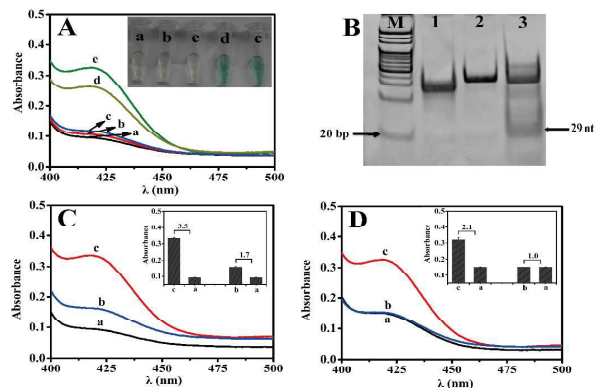
Fig. 1 (A) UV-vis absorbance spectra of (a) hemin + $ABTS^{2-}$-H_2O_2, (b) hemin + H1 + $ABTS^{2-}$-H_2O_2, (c) hemin + H1 + H2 + $ABTS^{2-}$-H_2O_2, (d) The purified SDA products + H1 + hemin + $ABTS^{2-}$-H_2O_2, (e) The purified SDA products + H1 + H2 + hemin + $ABTS^{2-}$-H_2O_2 (insets: the corresponding photographs) (5 nM miRNAs used in this case). (B) The native PAGE analysis: M: 20 bp DNA Ladder Marker, lane 1: Blank, lane 2: MB + miRNAs + Klenow fragment, lane 3: SDA. (C) UV-vis absorbance spectra of (a) purified SDA products (no miRNAs) + CHA, (b) purified SDA products (50 fM miRNAs) + CHA, (c) purified SDA products (5 nM miRNAs) + CHA (inset: the corresponding signal to noise). (D) UV-vis absorbance spectra of (a) no purified SDA products (no miRNAs) + CHA, (b) not purified SDA products (50 fM miRNAs) + CHA, (c) not purified SDA products (5 nM miRNAs) + CHA (inset: the corresponding signal to noise).

3.3. Optimization of experiment conditions

To obtain excellent analytical performance, different experimental parameters were optimized (Fig. 2). The signal-to-noise ratio was used to evaluate the performance of the nanomachine. The versatile MB acting as a template to initiate a SDA reaction greatly affected the machine performance. Therefore, the concentration of MB was firstly optimized. The signal-to-noise ratio increased as the increasing concentration of MB from 25 to 100 nM, then decreased from 100 to 150 nM (Fig. 2A), indicating that the more MB not only increased the machine signal but also enhanced the CHA "breathe" with the background increasing. Thus, 100 nM MB was used in all subsequent experiments. In addition, the time of SDA reaction also played an important role in the signal readout. At 100 nM MB, the highest signal-to-noise ratio was achieved at 80 min (Fig. 2B). Therefore, 80 min was adopted as the optimal SDA time.

To enhance detection sensitivity, H1 concentration and the incubating temperature of CHA reaction were also optimized. As shown in Fig. 2C, with the increasing concentration of H1 at 50 nM H2, the signal-to-noise ratio also increased and tended to decrease at 75 nM, indicating that the higher concentration of H1 not only increased the catalyzed reaction of target miRNAs but also increased the nonspecific CHA products for the breathing reaction of H1 and

H2. The incubating temperature was also investigated from 4 to 65 °C (Fig. 2D). At 37 °C, the signal-to-noise ratio reached the maximum, because the incubating temperature affected the stability of the hairpins. At low temperature, H1 and H2 could not obtain a sufficient collision probability that significantly decreased the formation of H1-H2 duplexes. And at high temperature, nonstable hairpins lead to a mass of nonspecific products.
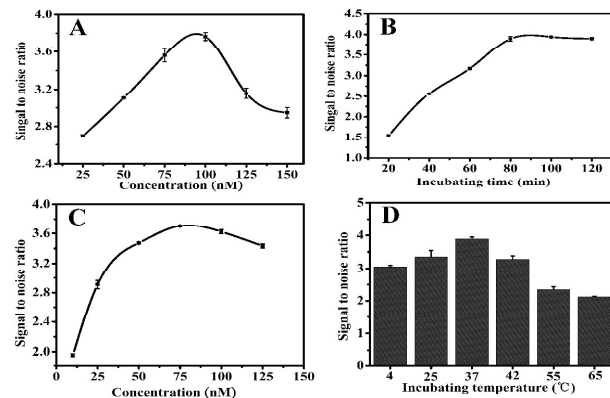
Fig. 2 Dependences of the signal-to-noise ratio on versatile MB concentration (A), SDA time (B), H1 concentration at H2 concentration of 50 nM (C), and incubating temperature of CHA reaction (D), when one parameter changes while the others are under their optimal conditions.

3.4. Analytical performance of the colorimetric nanomachine

Under the optimal experimental conditions, analytical performance of the colorimetric nanomachine was evaluated toward synthetic miRNAs standards at various concentrations. The absorbance increased with the increasing target miRNAs concentration (Fig. 3A). The plot of the response vs the logarithm of miRNAs concentration showed a good linear relationship in the range from 5 fM to 5 nM with a correlation coefficient of 0.9971 (Inset). Additionally, the limit of detection (LOD) was 1.7 fM at a signal-to-noise ratio of 3, which was much lower than previous reported methods based on CHA.[27, 37-40] For comparison, we also investigated the analytical property of the CHA reaction alone. The assay was carried out using the same protocol. As shown in Fig. 3B, the linear range and LOD were 2 pM-10 nM and 1.5 pM (S/N=3), respectively. As a result, the LOD of using SDA-CHA was approximately 3 orders of magnitude lower than that of using CHA alone. The achieved high sensitivity could be attributed to dual signal amplifications of the purified SDA and CHA. Thus, this versatile colorimetric biosensor might be applied to quantification of miRNAs with a wide linear range and low detection concentration.
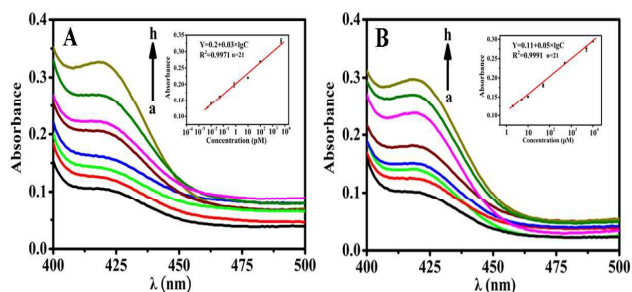
Fig. 3 (A) The absorbance curves responding to 0, 0.005, 0.01, 0.05, 0.75, 10, 100, 5000 pM target miRNAs (from a to h). Inset was corresponding calibration curves of the SDA-based DNA machine. (B) The absorbance curves responding to 0, 2, 5, 10, 50, 500, 5000, 1000 pM DNA catalyst (from a to h). Inset was calibration curves of the alone CHA. The error bars represented the standard deviations calculated from three different spots.

3.5. Versatility and specificity of the established machine

To evaluate versatile performance of DNA machine for different miRNAs detection, the MB with various miRNA-recognition domains was designed for detection of miRNAs. As shown in Fig. 4A, the absorbance of the established DNA machine was monitored using miRNA-21, miRNA-17, and miRNA-222 at 5 nM, 10 pM, and 10 fM, respectively. The absorbance increased with the increasing miRNAs concentration, which was in good agreement with those obtained by Fig. 3A. Thus, these results indicated that the DNA machine might be applied to versatile detection of different miRNAs only changing miRNA-recognition domains.

Another question arose as to whether the versatile machine with definite miRNA-recognition domains possessed good specificity for miRNAs detection. The machine was investigated by measuring the absorbance for six types of miRNA sequences, including complementary target (miRNA-21), SM, DM, NC, miRNA-222, and miRNA-17 at 5 nM. As shown in Fig. 4B, the machine displayed high fidelity in discriminating perfectly complementary target and the mismatched strands or other miRNAs. The high sequence specificity could be attributed to the high affinity and unique specificity of the hairpin structure of MB. In addition, the reproducibility of the developed DNA machine was also investigated. Five replicate measurements of miRNA-21 at 5 nM, 10 pM, and 10 fM were performed and the variation coefficients were 1.9%, 4.7%, and 5%, respectively. Herein, the machine displayed good specificity and acceptable reproducibility for determination of miRNAs.
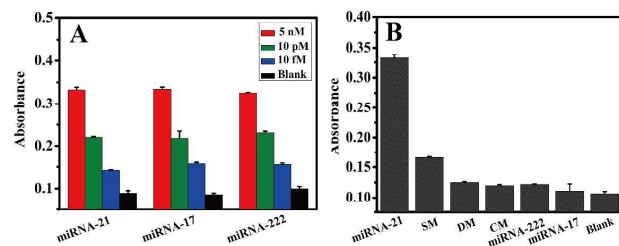
Fig. 4 (A) Versatility investigation of DNA machine for miRNA-21 (5 nM, 10 pM, 10 fM), miRNA-17 (5 nM, 10 pM, 10 fM), and miRNA-222 (5 nM, 10 pM, 10 fM). (B) Specificity investigation of DNA machine for 5 nM of miRNA-21, SM, DM, NC, miRNA-222, miRNA-17, and blank.

3.6. Real sample analysis

To evaluate the analytical feasibility and potential application of the developed machine, real sample analysis was performed using total RNA extracted from MCF-7 as an example (ESI). The total RNA was diluted to 400 ng/μL with DEPC-treated water, and 400 ng total RNA was used for detection. The absorbance generated by 200 ng of total RNA could be obviously distinguished from that generated by

the blank (Fig. 5). From the calibration curve (Fig. 3A), the amount of miRNA-21 in 400 ng total RNA sample was estimated to be 12.0 fM (RSD=9.7%, n=3). Furthermore, to further investigate analytical performance in real sample analysis, different amounts of miRNA-21 were spiked into 400 ng total RNA for the assay, and the results showed the recovery was in the range of 92.80%-100.70% (ESI, Table S2†), suggesting that the method could sensitively detect miRNAs in real samples with acceptable accuracy.
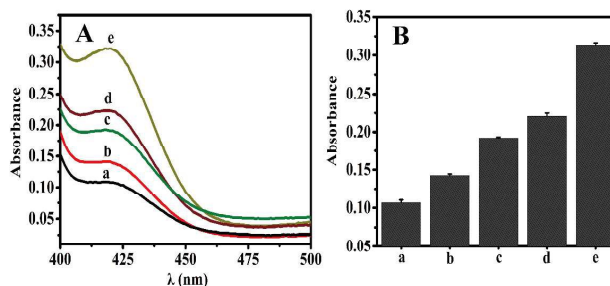
Fig. 5 (A) Application investigation of the developed machine for (a) blank, (b) miRNA-21 concentration of MCF-7 total RNA, (c) MCF-7 total RNA spiked with 500 fM miRNA-21, (d) MCF-7 total RNA spiked with 5 pM miRNA-21, (e) MCF-7 total RNA spiked with 5 nM miRNA-21. (B) The column diagram in accordance with results obtained by UV-vis absorbance spectra.

4. Conclusions

In summary, we have successfully established a novel and versatile DNA nanomachine for miRNAs determination based on SDA and CHA with DNAzyme formation. The developed nanomachine displays acceptable reproducibility, good specificity, and high sensitivity for miRNAs determination. Moreover, the detection limit of the colorimetric biosensor is as low as 1.7 fM, which is mainly attributed to the dual amplifications of SDA and CHA with DNAzyme formation and the purification of the SDA mixture for eliminating matrix interference. In addition, the versatile colorimetric biosensor can be applied to detect different miRNAs by only changing the miRNA-recognition domain of MB. Significantly, the established nanomachine can be easily extended for developing various biomolecules assay methods.

Acknowledgements

Notes and references

1   Y. Q. Wen, Y. Xu, X. H. Mao, Y. L. Wei, H. Y. Song, N. Chen, Q. Huang, C. H. Fan, D. Li, *Anal. Chem.* 2012, **84**, 7664-7669.
2   P. Zhang, X. Y. Wu, Y. Q. Chai, R. Yuan, *Analyst,* 2014, **139**, 2748-2753.
3   A. Lujambio and S.W. Lowe, *Nature*, 2012, **482**, 347-355.

4   S. M. Eacker, T. M. Dawson, V. L. Dawson, *Nat. Rev. Neurosci.,* 2009, **10**, 837-841.

5   R. J. Deng, L. H. Tang, Q. Q. Tian, Y. Wang, L. Lin, J. H. Li, *Angew. Chem. Int. Ed.,* 2014, **53**, 2389-2393.

6   G. L. Wang and C. Y. Zhang, *Anal. Chem.,* 2012, **84**, 7037-7042.

7   P. Shah, P. W. Thulstrup, S. K. Cho, Y. J. Bhang, J. C. Ahn, S. W. Choi, M. J. Bjerrum，S. W. Yang, *Analyst,* 2014, **139**, 2158-2166.

8   M. Selbach, B. Schwanhusser, N. Thierfelder, Z. Fang, R. Khanin, N. Rajewsky, *Nature*, 2008, **455**, 58-63.

9   D. P. Bartel, *Cell*, 2009, **136**, 215-233.

10 E. Varallyay, J. Burgyan, Z. Havelda, *Nat. Protoc., 2008,* **3**, 190-196.

11 J. M. Lee and Y. Jung, *Angew. Chem. Int. Ed.,* 2011, **50**, 12487-12490.

12 R. X. Duan, X. L. Zuo, S. T. Wang, X. Y. Quan, D. L. Chen, Z. F. Chen, L. Jiang, C. H. Fan, F. Xia, *J. Am. Chem. Soc.,* 2013, **135**, 4604-4607.

13 F. Ma, Y. Yang, C. Y. Zhang, *Anal. Chem.,* 2014, **86**, 6006-6011.

14 H. Zhou, J. Liu, J. J. Xu, H. Y. Chen, *Chem. Commun.,* 2011, **47**, 8358-8360.

15 L. J. Wang, Y. Zhang, C. Y. Zhang, *Anal. Chem.,* 2013, **85**, 11509-11517.

16 X. T. Liu, Q. W. Xue, Y. S. Ding, J. Zhu, L. Wang, W. Jiang, *Analyst,* 2014, **139**, 2884-2889.

17 S. Bi, Y. Y. Cui, L. Li, *Anal. Chim. Acta*, 2013, **760**, 69-74.

18 W. Cheng, F. Yan, L. Ding, H. X. Ju, Y. B. Yin, *Anal. Chem.,* 2010, **82**, 3337-3342.

19 H. Q. Wang, W. Y. Liu, Z. Wu, L. J. Tang, X. M. Xu, R. Q. Yu, J. H. Jiang, *Anal. Chem.,* 2011, **83**, 1883-1889.

20 M. Parida, G. Posadas, S. Inoue, F. Hasebe, K. Morita, *J. Clin. Microbiol.,* 2004, **42**, 257-263.

21 C. H. Luo, H. Tang, W. Cheng, L. Yan, D. C. Zhang, H. X. Ju, S. J. Ding, Biosens. Bioelectron., 2013, **48**, 132-137.

22 S. Cai, Y. H. Sun, C. W. Lau, J. Z. Lu, *Anal. Chim. Acta*, 2013, **761**, 137-142.

23 X. Zuo, F. Xia, Y. Xiao, K. W. Plaxco, *J. Am. Chem. Soc.,* 2010, **132**, 1816-1818.

24 M. J. Hall, S. D. Wharam, A. Weston, D. L. N. Cardy, W. H. Wilson, *Biotechniques*, 2002, **32**, 604-606.

25 Y. S. Jiang, B. L. Li, J. N. Milligan, S. Bhadra, A. D. Ellington, *J. Am. Chem. Soc.,* 2013, **135**, 7430-7433.

26 P. Yin, H. M. T. Choi, C. R. Calvert, N. A. Pierce, Nature, 2008, **541**, 318-323.

27 H. L. Li, J. T. Ren, Y. Q. Liu, E. K. Wang, *Chem. Commun.,* 2014, **50**, 704-706.

28 Z. Zhu, J. P. Lei, L. Liu, H. X. Ju, *Analyst*, 2013, **138**, 5995-6000.

29 B. L. Li, Y. S. Jiang, X. Chen, A. D. Ellington, *J. Am. Chem. Soc.,* 2012, **134**, 13918-13921.

30 S. F. Liu, Y. Wang, J. J. Ming, Y. Lin, C. B. Cheng, F. Li, *Biosens. Bioelectron.,* 2013，**49**, 472-477.

31 M. N. Stojanovic, P. de Prada, D. W. Landry, *Chem. Bio. Chem.,* 2001, **2**, 411-415.

32 P. Silverman and E. T. Kool, *Chem. Rev.,* 2006, **106**, 3775-3789.

33 B. L. Li, A. D. Ellington, X. Chen, *Nucleic Acids Res.*, 2011, **39**, e110.

34 S. Bhadra and A. D. Ellington, *Nucleic Acids Res.,* 2014, **42**, e58.

35 Y. S. Jiang, S. Bhadra, B. L. Li, A. D. Ellington, *Angew. Chem. Int. Ed.,* 2014, **126**, 1876-1879.

36 X. Chen, N. Briggs, J. R. McLain, A. D. Ellington, *Proc. Natl. Acad. Sci. U. S. A.,* 2013, **110**, 5386-5391.

37 J. Y. Zhuang, W. Q. Lai, G. N. Chen, D. P. Tang, *Chem. Commun.*, 2014, **50**, 2935-2938.

38 Y. H. Liao, R. Huang, Z. K. Ma, Y. X. Wu, X. M. Zhou, D. Xing, *Anal. Chem.* 2014, **86**, 4596-4605.

39 Y. Zhang, Y. R. Yan, W. H. Chen, W. Cheng, S. Q. Li, X. J. Ding, D. D. Li, H. Wang, H. X. Ju, S. J. Ding, *Biosens. Bioelectron.* 2015*,* **68**, 343-349.

40 A. X. Zheng, J. Li, J. R. Wang, X. R. Song, G. N. Chen, H. H. Yang, *Chem. Commun.,* 2012, **48**, 3112-3114.

Analyst Accepted Manuscript